Moroccan Journal of Chemistry
ISSN: 2351-812X
http://revues.imist.ma/?journal=morjchem&page=login
El Fels & al./ Mor. J. Chem. 5 N°4 (2017) 730-739

Assessment of organo-mineral fraction during co-composting of sewage sludge-lignocellulosic waste by XRD and FTIR analysis

Loubna El Fels[a,b*], Mohamed Zamama[c], Anas Aguelmous[d], Bouchra El Hayany[b], Ghizlen El Mezouari El Glaoui[b,e] Abdelhafid Benksim[f], Ilyesse Rahhou[j], Abdelfetah Mounir[f], Hassan Khajmi[f], Mohammed Rihani[e], Mohamed Hafidi[b]

[a] *Higher Institute of Nursing Professions and Health Technics, Marrakech-Safi, Morocco*
[b] *Laboratory of Ecology and Environment (L2E) (Unit Associated with the CNRST, URAC32), Faculty of Science Semlalia, Cadi Ayyad University, BP: 2390, Marrakech, Morocco*
[c] *Laboratory of Physico-Chemical of Materials and Environment (LPCME), Faculty of Science Semlalia, Cadi Ayyad University, BP: 2390, Marrakech, Morocco*
[d] *Laboratory of Process Engineering and Environment, Faculty of Science & Technology, Hassan II of Casablanca University, Morocco*
[e] *Laboratory of Marine Biotechnology and Environment, Faculty of Science, Chouaib Doukkali University El Jadida, Morocco*
[f] *Higher Institute of Nursing Professions and Health Technics, Marrakech, Morocco*
[j] *Higher Institute of Nursing Professions and Health Technics, Oujda, Morocco*

** Corresponding author:*
loubna.elfels@gmail.com
Received 06 March 2017,
Revised 17 September 2017,
Accepted 22 Sept 2017

Abstract

This investigation focuses mainly on highlighting the contribution of the IR spectrum of the mineral matrix in co-composts after removing the organic phase by slow pyrolysis. The mineral matrix is still confusion subject in the interpretation of FTIR spectra of co-composts. The XRF and XRD analysis of the low pyrolysis substrates of sewage sludge and date palm waste during six months of co-composting, show that the mineral fraction is homogeneous in the samples and that the inorganic matrix consists mainly of silica and carbonates including a residual portion remaining after pyrolysis. The comparison of FTIR spectra of heated samples at 105°C and 650°C shows that the 3500-3280 cm^{-1} region characterises essentially the hydroxyl groups OH ($\nu_{(OH)}$) of water molecules. The observed bands in this region provide information on the co-compost hydrophilic nature but can only provide limited information about the humic substances composition. The band at 1035 cm^{-1}, assigned commonly to organic material, which persists after the thermal treatment, should be assigned for the Si-O vibration of silica.

Keywords: *:* mineral matrix, thermal treatment, Co-composting, Si-O vibration, sludge pyrolysis, XDR and FT-IR.

1. Introduction

Wastewater treatment plant produces considerable quantities of sewage sludge. The possibility of sludge evacuation is limited and the problem increases with the underestimated solutions taken into account when wastewater plants are being designed. The composting process is one of the best waste treatment technology which facilitates the recycling of organic matter, especially sewage sludge, which is biologically degraded by micro-organisms to humus-like substances (HS). These end products are one of the keys used to identify the composting substrates maturity [1, 2, 3]. Several pathways were proposed to explain and understand the humification mechanisms. Chefetz et al. [4] showed that the biodegradation followed by an accumulation of recalcitrant compounds is one way for HS formation. A second mechanism, during which the polyphenols undergo a condensation and accumulation, was proposed by [5, 6]. A new hypothesis was provided; it involves a selective preservation of resistant aliphatic hydrocarbons formed during microbial biosynthesis [7]. Regardless of the following mechanism, the composition of the formed HS is linked to the starting raw matter and the humification conditions during the process [8]. Various spectroscopy and analytical methods (EPR, UV / VIS, ^{13}C NMR, and FTIR) are used to characterise and study the properties of substances formed by the humification process. The FTIR spectroscopy is one of the techniques largely used to study different samples without any previous chemical treatment likely to cause inappropriate reactions. Furthermore, this technique is widely used to characterise the evolution of organic substrates, mainly humic acid (HA) extracted from sewage sludge and bottom sediments [9], HS fraction extracted from the soil and from composted waste, such as sewage sludge [3, 10]; In addition to identifying the functional groups by their frequencies characteristic, it is possible to follow the HS composition by comparing the relative intensities of some absorption bands [11, 12]. The disappearance or the appearance of new bands in the FTIR spectrum provides information about the matter evolution and its interaction with heavy metals when they are present in sewage sludge [13, 14, 15, 16]. However, the indexing of FTIR spectra at different stages of the composting sewage sludge and palm waste evolution remains complicated considering the overlap of mineral phase bands with those of organic matter of the HS. In this case, it is difficult to attribute accurately the FTIR spectrum absorption bands in the 3500-3280 cm^{-1} and 1200-1000 cm^{-1} regions. As reported by [10, 17] in the case of HS extracted from compost, even after their purification, there often remains a relatively large portion of the mineral fraction that provides characteristic bands in FTIR spectrum that overlap with those of HA. The profile and position of the observed bands in these regions of the FTIR spectrum vary from one investigation to the another, and various attributions were made: (i) the broad and intense asymmetrical band appearing toward the 3450-3280 cm^{-1} was attributed to stretching vibrations of the OH groups bound by hydrogen bonding and NH groups of HA extracted from soil or sewage sludge [8, 9, 18]. (ii) the bands appearing in the 1200-1000 cm^{-1} region, in the HA sewage sludge spectrum have been the subject of various attributions. According to [9], these bands were attributed to aromatic ethers stretching vibration or to the Si-O; likewise to the stretching vibration of C-O-C in the carbohydrates, or to aromatic ethers and polysaccharides [16, 19, 20, 21]. Furthermore, Laurent et al. [22] attribute it to the OH stretching vibration. More specifically, Smikovic et al. [23] attribute the band at 1035 cm^{-1} to the mineral matter fraction in case its intensity and its frequency remain stable after thermal destruction of soil organic matter by heating at 225°C. The literature data show that the bands situated at 3500- 3280 cm^{-1} and 1200-1000 cm^{-1} of the FTIR spectrum characterise both the mineral fraction and the organic substances. However, the heated matter at 225°C does not confirm the total organic matter elimination in order to assign the residual FTIR spectrum bands especially to the mineral phase. In fact, thermal changes of sewage sludge fractions are complex and a number of successive reactions are involved. Those reactions depend on the sewage components and the thermal conditions, such as heating rate, duration, temperature, oxygen availability and the rehydration of the sample during the cooling. Current studies on thermal threatment are focused mainly on studying: (i) the mineralogical analysis of the impact of incineration conditions of paper mill sludge

on its compatibility with the Portland cement [24], (ii) volatile chemicals and pathogens removal by brief and intense heating systems, in order to obtain a disinfected end products [25], (iii) the tubular pyrolyzer for the dried products in order to explore and analyse the gases production and organic volatile compounds by thermogravimetric–FTIR [26]. Studies on the calcination of composting substrates, in order to emphasise on the contribution of the inorganic matrix in the FTIR spectrum, were not widely discussed. The main objective of this study is to emphasise on the contribution of the mineral matrix to the FTIR spectrum in a co-composting sewage sludge and waste palm after effective removal of the organic phase by slow pyrolysis.

2. Material and Methods

2.1. Sampling and co-composting trial

Sewage sludge from Marrakech treatment plan was composted with palm waste as follows: sewage sludge/ palm waste 50/50 (v/v), as mentioned in previous studies [27]. During co-composting process, the homogeneous samples (1 Kg) (0, 1, 2, and 6 months) were obtained by carefully mixing of several sub samples taken at different windrow point and quartering. The main physico-chemical parameters of co-composting substrates are presented in table 1.

Table 1: Main features of co-composted substrates according to [27]

Parameters	Sludge	Palm date waste
pH	6.45 ± 0.09	6.31 ± 0.08
Moisture (% FWt)	46.46 ± 0.26	25.10 ± 0.21
Ash content (% DWt)	43.80±0.02	9.0 ± 0.1
TOC (% DWt)	31.20 ± 0.11	50.5 ±0.6
KTN (% DWt)	1.50 ± 0.2	1.36 ±0.24
C/N	20.8	37.13

FWt: Fresh weight; DWt dry weight; TOC: total organic carbon; KTN: Kjeldahl total nitrogen

2.2. Thermal treatment

Previously dried samples were thermally treated by pyrolysis in ceramic pots on a fixed bed using a muffle furnac (FERRO). The temperature rise is linear and was programmed at 5°C / min up to 650°C, at this temperature the calcination of the samples holds about 6 hours. The cooling is carried out at closed oven.

2.3. Chemical analysis by X-ray fluorescence (XRF)

The analyses of the chemical composition of the compost samples calcinated at 650°C were performed by a X-ray fluorescence spectrometer (Pioneer XRF-S4) using Spectra PLUS software with the Eval interactive evaluation.

2.4. XRD analysis

Dried samples at 105°C and the calcinated samples at 650°C were milled and analysed by the diffraction technique, using the (diffractometre) Philips X'PERT, a copper anticathode wavelength $\lambda = 1.540560$ Å operating at 40kV and 40mA. The data acquisition is carried out by a control unit for angles 2 theta (2θ) between 5 and 70° diffractograms processing were performed using the X'Petrt HighScore software. The indexing phase is based on the comparison of the XRD database ASTM (American Society for Testing and Materials) by comparing the inter-reticular distances of d to angles 2θ. The database used for the identification of the phases is PDF2 (2004) Converted High Score-Banc.

2.5. Fourier transform infrared spectroscopy (FTIR) analysis

Each treated sample (at 105°C and 650°C) was mixed with dried potassium bromide (Kbr) with a (sample/ Kbr, 2:200 mg) ratio. The mixture is then compressed under vacuum. The pellets were analysed covering a frequency range of 4000-400 cm^{-1} using a Bruker Vertex 70 FTIR spectrometer equipped with a DTGS detector and OPUS software 6.5 (128 scans at a resolution of 2 cm^{-1} were carried out). The spectral data are obtained as values of absorbance.

3. Results and Discussion

3.1. XRF elements composition analysis

Table 2 present the XRF results. The main elements present in different co-composting stages are presented as oxides form. It was noted that the composition is homogeneous. The different co-composted samples are poor in aluminium. However, silicat and carbonat exhibit a high level. During co-composting, the total content of metallic trace elements (MTE) such as copper, zinc, lead and chromium is low. These results confirm the sludge sandy texture and the low clay character. A relatively large proportion of phosphate and potassium is present. Towards the end of the co-composting, the total of mineral elements increases and the rate of the organic material decreases. The ignition loss is high for all samples ranging from 55.82 to 56.08% that indicates a significant rate of organic matter in the compost.

Table 2: Chemical composition using X-ray fluorescence analyses

Components	Calcinated samples			
	Co-composting time (months)			
	0	1	2	6
SiO_2	17.84	19.30	20.30	19.32
Al_2O_3	5.60	4.72	4.04	4.37
Fe_20_3	1,05	0.88	0.76	0.80
MgO	2.98	3.36	3.76	3.44
CaO	7.63	6.77	6.17	6.43
Na_2O	0.67	0.74	0.77	0.77
K_2O	1.33	1.76	1.95	1.92
TiO_2	0.17	0.13	0.10	0.13
P_2O_5	3.03	2.70	2.36	2.45
SO3	2.86	2.61	2.59	2.96
Cl	0.51	0.94	1.22	1.27
Cr_2O_7	0.02	0.02	0.02	0.02
MnO	0.02	0.02	0.02	0.02
ZnO	0.04	0.03	0.03	0.03
CuO	0.01	0.01	0.01	0.01
PbO	0.01	0.01	0.00	0.01
Total mineral	43.76	43.99	44.10	44.94
Ignition loss	56.13	55.82	54.92	56.08
Total	99.89	99.81	99.02	100.02

3.2. XRD mineralogical analysis

The XRD patterns of heated sample at 105°C (Figure 1) show the presence of amorphous or poorly crystallized phases. Nevertheless, at (2θ =15-25), a characteristic peak of cellulose fibers (Cel) was observed.

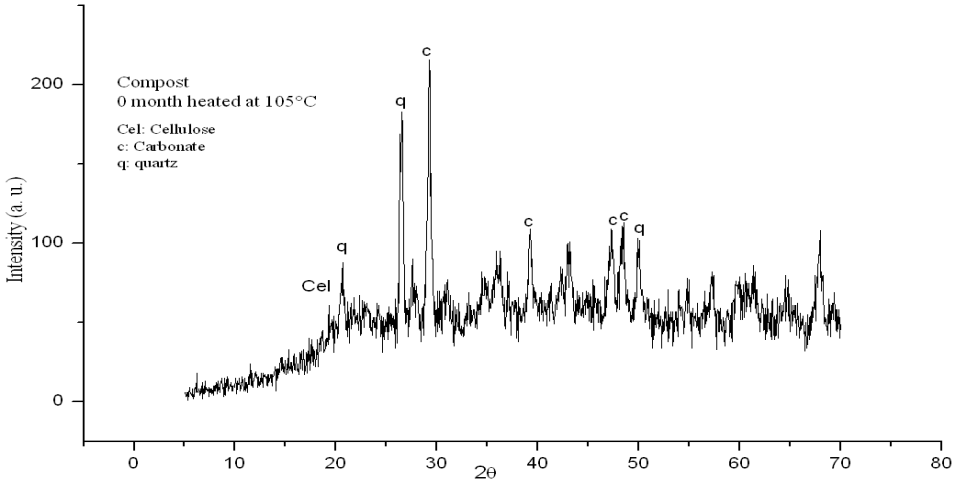

Figure 1: DRX analyses of dried compost samples at 105 °C

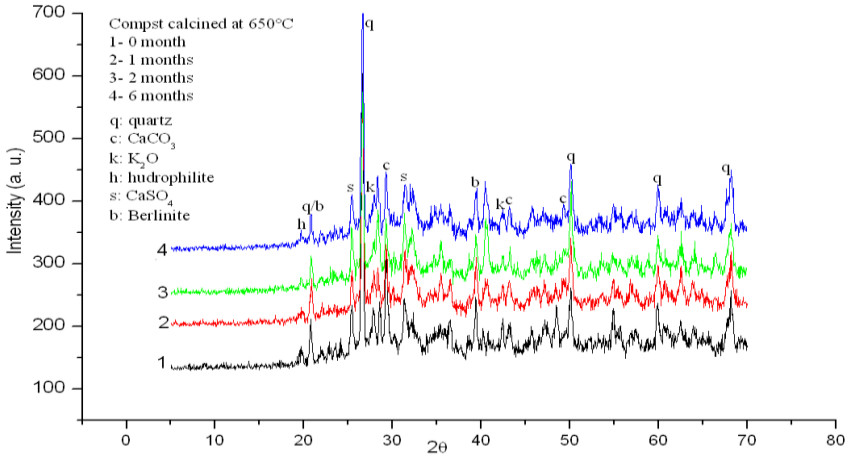

Figure 2: DRX analyses of calcinated compost samples at 650°C

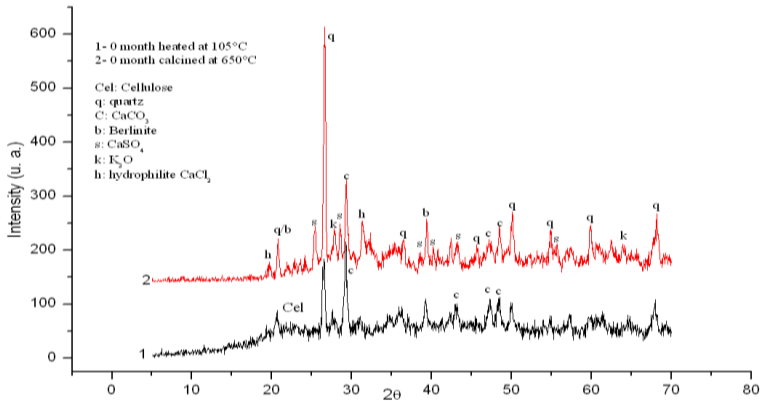

Figure 3: DRX comparison between compost samples before and after calcination

The cellulosic compounds are linear biopolymers of anhydrocglucose, which by their hydrogen bonding lead to cellulose crystallised forms. The crystal structure is characterised by a large band in the region (2θ = 21.3-22.6) corresponding to the 002 diffraction plane [28]. The XRD analysis of the samples thermally treated at 105° C and

650° C (Figure 2) have the same profile. However, at 650 °C, the characteristic peak of cellulose disappears completely. These results are in agreement with the studies on cellulose thermal degradation, ranging from 390 to 600°C. Nevertheless that is linked to inorganic fraction rate [29]. Moreover, by comparison with quartz peak (2θ = 25-30 region), the XRD of calcinated samples show a clear decrease of carbonates which are not completely eliminated at this temperature (Figure 2, 3). After calcination at 650°C no new phase was observed by DRX. Residual peaks indexed taking into account the composition given by XRF showed that the present phases are silica, calcium as hydrophilite carbonat forms ($CaCl_2$), sulphate ($CaSO_4$), and phosphorus that is probably as berlinite ($AlPO_4$). This could explain that overall organic matter degraded at 650°C and only mineral fraction persists

3.3. FTIR analysis

The FTIR spectra of all samples (Figure 4) showed that no bands were observed in the 3600-3700 cm^{-1} region. This spectrum region characterises the phylloscilicate phases as kaolins, micas and illite. These results are in agreement with the XRD analysis, which showed no peak at low values of θ, and with the XRF data, which show a high percentage of silica compared to alumina that could explain the silicate composition of co-composted substrates.

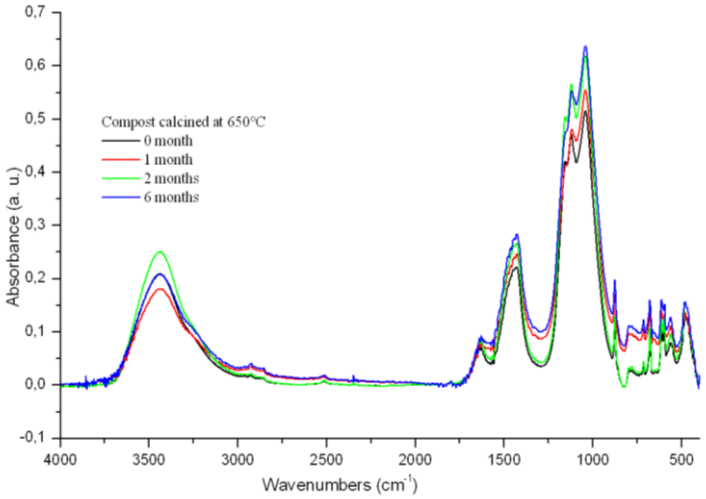

Figure 4: IR spectra of calcinated compost samples

The thermal treatment causes significant changes in intensities and positions of the absorption bands. Compared with the spectrum of the heated sample at 105°C (Figure 5, Table 3), the FTIR spectra of the calcinated samples at 650°C show:

- A decrease in intensity of the bands of stretching vibration of OH groups, which are located at 3406 cm^{-1} and 3280 cm^{-1}.
- The total disappearance of the epaulement located at 1236 cm^{-1}, and the bands located in the region 3000 to 2800 cm^{-1}, which are characteristic of aliphatic C-H groups. That is due to the degradation of organic matter by pyrolysis. Fernández et al. [30] attributed the bands located at 2535, 1795, 1435 and 875 cm^{-1} to calcite compounds.
- A decrease of the intensities of bands situated at 2535, 1795, 1435 and 875 cm^{-1}. These frequencies are typical for calcite. The persistence of some epaulements at 650°C shows that the carbonates are not completely degraded.
- The persistence of two intense bands located in the region 1155-1035 cm^{-1}, are characteristic of silica.

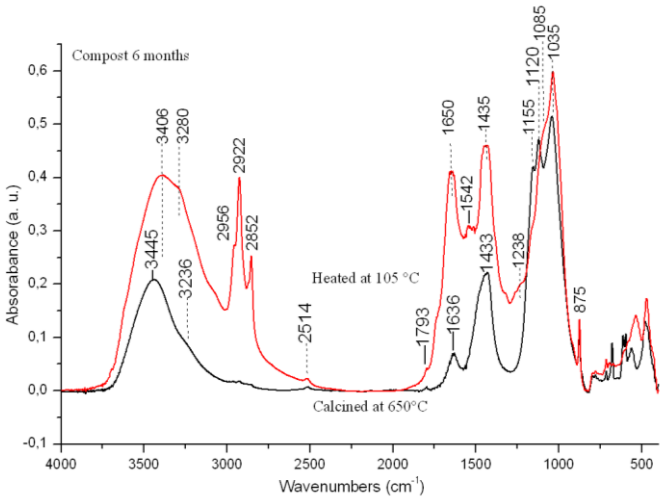

Figure 5: IR spectra comparison between compost samples before and after calcination

The FTIR spectra show that the calcination of samples causes on one hand, a complete disappearance of some bands. That could explain that thermal treatment removes the phases associated with these bands. On the other hand, the thermal treatment causes the decrease in the intensity of some bands, which remain located on the same wavenumbers. However, others bands are dislocated and decrease in intensity such as the bands at 3406, 3280, 1650 and 1085 cm^{-1} which are dislocated respectively to 3445, 3236 1636 and 1120 cm^{-1} after calcination (Figure 5). The organic matter rate, temperature, heating period, availability of oxygen and the hydration rate of the sample during cooling could explain these data. The literature data show different conditions to specific degradation of organic matter, nevertheless the phenomena that occur during the calcination are still controversial. Fernandez et al. [31] showed over than 75% of the holocellulose losses from two different humic soils at 220°C; and the lipidic fraction exhibited different thermal resistance in both soils, showing losses of 73% in one case and only 11% in the other. However at 350°C, holocellulose practically disappeared and lignin losses were significant. In another study, heating at 225 ° C for 5 hours led to a reduction of 13% of organic substances [23]. The low pyrolysis used in the gasification of wood at 450°C for 2 hours, occurs the degradation of cellulose and lignin; and the remaining residue is composed primarily of coke and mineral [32]. A Recent thermogravimetric study [26], shows that between 276 and 454°C, there occurs not only proteins and carboxyl groups decomposition but also the cracking of carbon refractories such as aromatic ring, N-alkyl long chain structures and some saturated aliphatic chains [17, 26]. At temperature range 492-720°C, the mass loss observed was attributed to the decomposition of inorganic materials such as calcium carbonate [33]. However, Frías et al. [34] showed that the calcination at 650°C for 2 h leads to the total destruction of organic fibers, and a low decarbonatation of calcite. That could explain that organic matter fraction is completely degraded at 650°C for 5 hours. Our FTIR analysis spectra are based on the assumption that the residual bands characterize only the mineral matrix. The asymmetric band in the region 3500-3280 cm^{-1} of the dried sample at 105°C, could point two components located at 3406 cm^{-1} and 3280 cm^{-1}, which their intensity decreased and dislocated respectively to 3445 and 3236 cm^{-1} after pyrolysis (Figure 5, Table 3). It was showed also that the band located at 1636 cm^{-1} persists after calcination. Similar bands were observed at 3443 and 1632 cm^{-1} in the IR spectrum of paper sludge pyrolysed, which have been respectively assigned to the stretching vibrations of hydroxyl water $\nu_{(O-H)}$ and its deformation ($\delta_{(HOH)}$) [30]. Several authors attributed these bands to water molecules which are interacting, but are not able to develop extensive chains or networks such as hydrated smectites at 3450, and 3350 cm^{-1} [35]; water in the H_2O/AOT/i-octane micelles, at 3455, and 3290 cm^{-1} [36], water in polyvinyl chloride polymers and the polythene tetraphthalate at 3510 and 3380 cm^{-1} [37]. Clegg et al. [38] demonstrated that a rehydration phenomenon occurs during cooling of clays previously heated at

500°C in air or in controlled atmosphere. That could explain the dislocation of the band from 3406 to 3445 cm^{-1} after pyrolysis at 650°C (Table 3). The other bands located at 3430 cm^{-1} and 3260 cm^{-1} disappear almost completely at 400°C.

Table 3 : Characteristic bands of sludge mineral matrix

Wavenumbers (cm^{-1})		Attributions
Dried samples at 105°C	Calcinated samples at 650°C	
3405	3445	Water stretching ν_{O-H}
3280	3236	Water combination $2\delta_{H-O-H}$
2535, 1795, 1435 et 875	1435, 875	Carbonates vibration
1155	1155	Silica vibration
1080	1120	Silica vibration
1035	1037	Si-O vibration

A rehydration phenomenon occurs during cooling of the sample allows the appearance of a band located at 3450 cm^{-1}, higher than that of unheated sample (3430 cm^{-1}). The other band appeared at the same wavenumber as the starting sample 3260 cm^{-1}. These bands have been attributed to water molecules that associate with phases resulting from the heat treatment. It was noted that the hydroxyl behaviour before and after calcination of our samples is similar to hydroxyl in the major minerals involved in the chemical and mineralogical transformation of hydrated phases during their calcinations. In the event that the potential function describing these water molecules is similar to that of the hydrated phases, we assign the band at 3406 cm^{-1}, on the FTIR spectrum of the dried samples at 105°C, to stretching vibration $\nu_{(O-H)}$ of hydroxyl groups of water molecules. The masked band by the presence of the organic matter contained in the dried sample at 105°C and which is highlighted at 1636 cm^{-1}, could be attributed to the deformation mode ($\delta_{(HOH)}$) after calcination. As to the component located at 3280 cm^{-1} on the dried sample spectrum, and which is dislocated after calcination to 3236 cm^{-1}, is probably due to a combination of the deformation mode ($\delta_{(HOH)}$) observed at around of 1636 cm^{-1}.In the region 1200-1000 cm^{-1}, we identified a poorly resolved massif consists of two bands located at 1155 and 1080 and 1035 cm^{-1}. Those bands are located at 1150, 1120 and 1037 cm^{-1} after calcination. Similar bands were observed at 1150 and 1080 cm^{-1} in the case of amorphous silica [30]. It is likely that the heat treatment promotes the crystallization of the amorphous silica which results in the appearance of well-resolved bands located at the same frequency as those found on the FTIR spectrum of the quartz [31]. These data are in agreement with the results of the composition obtained by XRF, which show the existence of the major mineral phases of silicate nature. The FTIR spectra are also in agreement with the XRD diagrams, which show a better crystallisation after pyrolysis. The band at 1035 cm^{-1} (located at 1037 cm^{-1} after calcination) is insensitive to the pyrolysis that could be attributed to Si-O vibrations of the silica present in the samples (Table 3). The presence of similar bands in this region of the FTIR spectrum is very common when the IR spectrum is recorded from a soil, which not has been subject of a specific extraction method [17, 39]. Even after HA extraction, a rat of about (6.35% Ash) of mineral fraction remains. A dislocated band at 1035 cm^{-1} was attributed to Si-O vibrations of clay impurities and indicates the presence of clay material, which is not completely removed during the purification process [8, 40].

4. Conclusion

Assessment of organo-mineral fraction during six months of co-composting of sewage-lignocellulosic waste by FTIR analysis was investigated. The XRD data show a series of diffraction peaks corresponding to the crystallised phases

and background noise whose form indicates the presence of poorly crystallised phases. The silica, calcite, and quartz are the main compounds of mineral fraction of co-composted substrates. This result shows that the samples taken at different stages of co-composting seem to have the same mineral composition. FTIR spectroscopy analysis, shows that the region 3500-3280 cm^{-1} is characteristic of water molecules. The appearing inorganic, wide and intense bands in this region hide the organic matter footprint. Nevertheless, this region indicates of the organic matter and its ability to interact with water molecules thus causing the movement of ν_{OH} characteristics of the water molecules, and the water molecules of organic matter. Consequently, the data in this region provide information on the interaction between organic matter and water molecules. However information on the composts organic matter composition is limited. The spectrum region 1200-1000 cm^{-1} characterises especially sewage sludge silica. The identified fine and intense band at 1035 cm^{-1} is attributed to Si-O. With important molar extinction coefficient, its intensity even at heat treatment suggests the opportunity of using this band as internal standards for semi-quantitative studies on the organic matter evolution during co-composting.

References

[1] F.J. Stevenson, X.T. He, Soil Science Society of America and American Society of Agronomy, Madison, Wisconsin, 91 (1990) –109.

[2] A. Ouatmane, M.R. Provenzano, M. Hafidi, N. Sensi, Compost Science & Utilisation. 8 (2000) 124-134.

[3] F.S. Higashikawa, C.A. Silva, C.A. Nunes, M.A. Sánchez-Monedero, Science of the Total Environment. 470 (2014) 536–542.

[4] B. Chefetz, Y. Chen, E. Clapp, P.G. Hatcher, Soil Sci. Soc. Am. J. 64 (2000) 583-589.

[5] W. Flaig, Effects of microorganisms in the transformations of lignin to humic substances, Geochim & Cosmochem Acta. 28 (1964) 1523–1535.

[6] A. Veeken, K. Nierop, V. de Wilde, B, Hamelers, Biores Technol. 72(2000) 33–41.

[7] E. Lichtfouse, C. Chenu, F. Baudin, C. Leblond, M. Da Silva, F. Behar, S. Derenne, C. Largeau, P. Wehrung, P. Albrecht, Org. Geochem. 28 (1998) 411–415.

[8] M. González Pérez, L. Martin-Neto, S.C. Saab, E.H. Novotny, D.M.B.P. Milori, V.S. Bagnato, L.A. Colnago, W.J. Melo, H. Knicker, Geoderma. 118 (2004) 181–190.

[9] J. Polak, M. Bartoszek, W.W. Sułkowski, J. Mol. Structure. 924 (2009) 309-312.

[10] M. Kaiser, R.H. Ellerbrock, Geoderma. 127 (2005) 196–206.

[11] B. Chefetz, T. Ilani, E. Schulz, J. Chorover, Water Sciences & Technology. 53 (2006) 51-57.

[12] S. Amir, M. Hafidi, L. Lemee, J.R. Bailly, G. Merlina, M. Kaemmerer, J.C. Revel, A. Ambles, J. Anal. Appl. Pyrolysis. 77 (2006) 149–158.

[13] J. Pajączkowska, A. Sułkowska, W.W. Sułkowski, M. Je¸drzejczyk, Journal of Molecular Structure. 651 (2003) 141–149.

[14] M., Jerzykiewicz, Formation of new radicals in humic acids upon interaction Pb(II) ions, Geoderma. 122 (2004) 305-309.

[15] J. Polak, W.W. Sułkowski, M. Bartoszek, W. Papiez, Spectroscopic studies of the progress of humification processes in humic acid extracted from sewage sludge, Journal of Molecular Structure. 744 (2005) 983–989.

[16] M.F. Sawalha, J.R. Peralta-Videa, G.B. Saupe, K.M. Dokken, J.L. Gardea-Torresdey, Chemosphere. 66 (2007) 1424–1430.

[17] G. Haberhauer, B. Rafferty, F. Strebl, M.H. Gerzabek, Geoderma. 83 (1998) 331–342.

[18] N. Senesi, V. D'Orazio, G. Ricca, Geoderma. 116 (2003) 325– 344.

[19] J. Niemeyer, Y. Chen, J.M. Bollag, Soil Sci. Soc. Am. J, 56 (1992) 135–140.
[20] A. Laguirtati, G. Ait Baddi, A. El Mousadik, A. Gilard, J.C. Revel, M. Hafidi, International Biodeterioration & Biodegradation. 56 (2005) 8–16.
[21] B.E. Madari, J.B. Reeves III, P.L.O.A. Machado, C.M. Guimarães, E. Torres, G.W. McCarty, 136 (2006) 245–259.
[22] J. Laurent, M. Pierra, M. Casellas, C. Dagot, Chemosphere. 77 (2009) 771-777.
[23] I. Simkovic, P. Dlapa, S.H. J. Doerr Mataix-Solera, V. Sasinkova, Catena. 74 (2008) 205-211.
[24] D.C. EL Ouazzani, A. Bouamrane, K. Mansouri, C.B. Fokam, J. Mater. Environ. Sci. 3 (2012) 628-635.
[25] J.M. Fernandez, N. Sensi, C. Plaza, G. Brunetti, A. Polo, Pedosphere. 19 (2009) 281–291.
[26] N. Gao, J. Li, B. Qi, A. Li, Y. Duan, Z. Wang, Journal of Analytical and Applied Pyrolysis. 105 (2014) 43-48.
[27] L. El Fels, M. Zamama, A. El Asli, M. Hafidi, International Biodeterioration & Biodegradation. 87 (2014) 128-137.
[28] C.F. Liu, F. Xu, J.X. Sun. J.L. Ren, S. Curling, R.C. Sun, P. Fowler, M.S. Baird, Carbohydrate Research. 341 (2006) 2677-2687.
[29] A. Mendez, J.M. Fidalgo, F. Guerrero, G. Gascó, J. Anal. Appl. Pyrolisis. 86 (2009) 66-73.
[30] R. Fernández, B. Nebreda, R.V. de la Villa, R. García, M. Frías, Cement & Concrete Composites. 32 (2010) 775–782.
[31] I. Fernandez, A. Cabeneiro, T. Carballas, Geoderma. 104 (2001) 281–298.
[32] D.J. Nowakowski, J.M. Jones, Journal of Analytical and Applied Pyrolysis. 83 (2008) 12-25.
[33] C. Casajus, J. Abrego, F. Marias, J. Vaxelaire, J.L. Sanchez, A. Gonzalo, Chemical Engineering Journal. 145 (2009) 412-419.
[34] M. Frías, R. García, R. Vigil, S. Ferreiro, Appl Clay Sci. 42 (2008) 189–193.
[35] J.L. Bishop, C.M. Pieters, J.O. Edwards, Clays Clay Miner. 42 (1994) 702–716.
[36] T.K. Jain, M. Varshney, A. Maitra, J. Phys. Chem. 93(1989) 7409–74016.
[37] C. Sammon, C. Mura, J. Yarwood, N. Everall, R. Swart, D. Hodge, J. Phys. Chem. B. 102 (1998) 3402–3411.
[38] F. Clegg, C. Breen, M.A. Carter, C. Ince, S.D. Savage, M.A. Wilson, J. Am. Ceram. Soc. 95 (2012) 416–422.
[39] R.H. Ellerbrock, H.H. Gerke, J. Bachmann, M.O. Goebel, Soil Science Society of America Journal. 69 (2005) 57–66.
[40] D.C. Olk, G. Brunetti, N. Senesi, Soil Sci. 164 (1999) 649 – 663.